Photosynthesis Research (2019) 140:221–233
https://doi.org/10.1007/s11120-018-0594-9

EMERGING TECHNIQUES

Maximum fluorescence and electron transport kinetics determined by light-induced fluorescence transients (LIFT) for photosynthesis phenotyping

Beat Keller[1,3] · Imre Vass[2] · Shizue Matsubara[1] · Kenny Paul[2] · Christoph Jedmowski[1] · Roland Pieruschka[1] · Ladislav Nedbal[1] · Uwe Rascher[1] · Onno Muller[1]

Received: 10 November 2017 / Accepted: 9 October 2018 / Published online: 24 October 2018

Abstract

Photosynthetic phenotyping requires quick characterization of dynamic traits when measuring large plant numbers in a fluctuating environment. Here, we evaluated the light-induced fluorescence transient (LIFT) method for its capacity to yield rapidly fluorometric parameters from 0.6 m distance. The close approximation of LIFT to conventional chlorophyll fluorescence (ChlF) parameters is shown under controlled conditions in spinach leaves and isolated thylakoids when electron transport was impaired by anoxic conditions or chemical inhibitors. The ChlF rise from minimum fluorescence (F_o) to maximum fluorescence induced by fast repetition rate (F_{m-FRR}) flashes was dominated by reduction of the primary electron acceptor in photosystem II (Q_A). The subsequent reoxidation of Q_A^- was quantified using the relaxation of ChlF in 0.65 ms (F_{r1}) and 120 ms (F_{r2}) phases. Reoxidation efficiency of Q_A^- (F_{r1}/F_v, where $F_v = F_{m-FRR} - F_o$) decreased when electron transport was impaired, while quantum efficiency of photosystem II (F_v/F_m) showed often no significant effect. ChlF relaxations of the LIFT were similar to an independent other method. Under increasing light intensities, F_{r2}'/F_q' (where F_{r2}' and F_q' represent F_{r2} and F_v in the light-adapted state, respectively) was hardly affected, whereas the operating efficiency of photosystem II (F_q'/F_m') decreased due to non-photochemical quenching. F_{m-FRR} was significantly lower than the ChlF maximum induced by multiple turnover (F_{m-MT}) flashes. However, the resulting F_v/F_m and F_q'/F_m' from both flashes were highly correlated. The LIFT method complements F_v/F_m with information about efficiency of electron transport. Measurements in situ and from a distance facilitate application in high-throughput and automated phenotyping.

Keywords Fluorescence transient · Photosynthesis · Fast repetition rate · Electron transport kinetics

Introduction

Photosynthetic processes, from light absorption by the chlorophyll-based pigments through charge separation in the photosystem II (PSII) reaction centers and sequential electron transport, are related to the redox state of the primary quinone electron acceptor (Q_A) and coupled to the signature of chlorophyll fluorescence (ChlF) (Kautsky and Hirsch 1931; Baker 2008; Müh et al. 2012). Based on ChlF, parameters such as the maximum quantum efficiency of PSII (F_v/F_m) and non-photochemical quenching (NPQ) estimating the proportion of absorbed light energy utilized for PSII photochemistry and non-photochemical energy dissipation, respectively, were established (Butler 1978; Baker 2008; Lazár 2013). The quick assessment of ChlF makes this signal a powerful tool for plant phenotyping (Furbank and Tester 2011; Fiorani and Schurr 2013). Phenotyping

Electronic supplementary material The online version of this article (https://doi.org/10.1007/s11120-018-0594-9) contains supplementary material, which is available to authorized users.

✉ Beat Keller
beat.keller@usys.ethz.ch

[1] Institute of Bio- and Geosciences, IBG-2: Plant Sciences, Forschungszentrum Jülich GmbH, 52425 Jülich, Germany

[2] Institute of Plant Biology, Biological Research Center, 6726 Szeged, Hungary

[3] Present Address: Molecular Plant Breeding, ETH Zürich, 8092 Zurich, Switzerland

requires characterization of a large plant set which needs to be completed before significant changes in the measured traits occur. This is particularly difficult when phenotyping photosynthesis because this process is highly dynamic and sensitive to environmental conditions (Ananyev et al. 2005a; Kono and Terashima 2014).

In order to determine F_v/F_m, the ChlF signal is compared under conditions when Q_A is in a fully oxidized state resulting in minimal ChlF (F_o) respective to the fully reduced state resulting in maximal ChlF (F_m). Two approaches using strong light pulses are widely accepted to reduce Q_A fully: the single turnover flash (STF) and the multiple turnover flash (MTF) (Kalaji et al. 2017). A saturating STF has to provide high enough excitation power to induce one single charge separation in all PSII reaction centers and fully reduce Q_A in order to yield maximum ChlF level (F_{m-ST}) (Malkin and Kok 1966; Schreiber 1986a; Samson and Bruce 1996; Kolber et al. 1998; Steffen et al. 2001). The excitation flash needs to be short enough (from fs to few µs) to prevent reoxidation of Q_A^- and reexcitation of PSII reaction centers (Malkin and Kok 1966; Belyaeva et al. 2014). In contrast, a saturating MTF requires at least 0.2-s duration of excitation at a few 1000 µmol photons m^{-2} s^{-1} (Ögren and Baker 1985; Schreiber et al. 1986b; Schreiber 2004). Within this time range, Q_A is reduced and reoxidized several times followed by reduction of the plastoquinone (PQ) pool and electron transfer to Photosystem I (PSI) (Vernotte et al. 1979; Schansker et al. 2005). MTFs ultimately result in an about 50% higher maximum ChlF level (F_{m-MT}) compared to F_{m-ST} (Schreiber 1986a; Schreiber et al. 1986b; Schansker et al. 2011). The difference between F_{m-ST} and F_{m-MT} was named the thermal phase because it is dependent on temperature, i.e., it is rate-limited (Delosme 1967). Later, the ChlF rise of the thermal phase was related to electron transport kinetics, particularly the accumulation of secondary quinone acceptors (Q_B) in a reduced state (Strasser et al. 1995; Lazár 2006). However, the origin of the thermal phase is not yet localized due to the complex and overlying kinetics of different electron transport processes (Rascher and Nedbal 2006; Müh et al. 2012) and the probable involvement of additional ChlF quenchers (Schansker et al. 2011, 2014; Prášil et al. 2018; Magyar et al. 2018).

Alternatively, electron transport kinetics in the dark-adapted state were studied by following reoxidation of Q_A^- coupled to ChlF relaxation after a STF (Vass et al. 1999; Petrouleas and Crofts 2005). According to an exponential decay model with three time constants, ChlF relaxes due to electron transport from Q_A^- to Q_B with a time constant (τ_1) of 0.1–0.2 ms when the Q_B site is occupied by a PQ (Bowes and Crofts 1980; Vass et al. 1999; Shinkarev 2004; Petrouleas and Crofts 2005). The second exponential component represents the reoxidation of Q_A^- which had initially no PQ molecule bound (Taoka and Crofts 1990; Petrouleas and Crofts 2005). Therefore, this time constant (τ_2) represents the binding of PQ molecule to the Q_B site of PSII and is estimated to be between 2.2 and 10 ms (Vass et al. 1999; Eshaghi et al. 2000). The third component (τ_3) is slow (500 ms to seconds) and interpreted as a back reaction from Q_A^- to the donor side components of PSII, specifically the S_2 state of the oxygen evolving complex (OEC) (Robinson and Crofts 1983; Vass et al. 1999). Most of the existing ChlF-based techniques apply STFs either from a measuring head in direct contact with the leaf surface, or from a few cm distance. F_{m-ST} is then recorded from a dark-adapted sample with an oxidized electron transport chain (Vernotte et al. 1979; Schansker et al. 2014). This allows standardized examination and modeling of ChlF relaxation kinetics in the dark (Vass et al. 1999). However, these requirements are impractical under conditions of ambient illumination, specifically when the presence of light is required for manifestation of stress conditions in the targeted plants. One such example is temperature stress, where low temperature enhances the photodamage effects of excess light (Pieruschka et al. 2010). In addition, the conventional fluorometric techniques may not provide sufficient resolution and throughput to capture highly dynamic regulation of photosynthesis.

The light-induced fluorescence transient (LIFT) method probes PSII from a distance using subsaturating (actinic) measuring flashlets in fast repetition rate (FRR) (Kolber et al. 1998; Osmond et al. 2017). In contrast to other techniques, no separate saturating flash is required in the LIFT method because the FRR probe flashlets are used directly for that purpose. The short measuring time of 0.2 s allows integration into automated systems for phenotyping in high spatio-temporal resolution. Following application in marine research (Kolber et al. 1998; Suggett et al. 2001; Oxborough et al. 2012; Robinson et al. 2014), a stationary LIFT system was installed for monitoring plant canopy from a distance of 50 m using laser excitation (Pieruschka et al. 2010, 2014; Raesch et al. 2014). Operating efficiency of PSII (F_q'/F_m') measured with this previous LIFT system correlated well with pulse amplitude modulation (PAM) measurements ($R^2 = 0.89$) and CO_2 assimilation rates ($R^2 = 0.94$) (Ananyev et al. 2005a; Pieruschka et al. 2010, 2014).

Here, we evaluated a newly developed LIFT device for its capacity to yield robust fluorometric parameters useful in plant phenotyping. Parameters as maximum ChlF induced by FRR flash (F_{m-FRR}) and Q_A^- reoxidation efficiency in 0.65 ms (F_{r1}/F_v) and 120 ms (F_{r2}/F_v) relaxation phases were introduced. The parameters were determined in isolated thylakoids and intact plants subjected to different treatments (electron transport inhibitors, anaerobiosis, or light) and approximated well-established ChlF parameters.

Materials and methods

Plant cultivation

In total, 36 spinach (*Spinacia oleracea*) plants of genotype *Matador* were grown in the greenhouse in Jülich, Germany, under 16-h/8-h day/night cycle at 20 °C/18 °C. Light intensity was kept automatically between 60 and 300 µmol photons m^{-2} s^{-1} using additional lamps or shading nets. 400-mL pots were filled with a turf-clay substrate (ED73, Einheitserdewerke, Sinntal-Altengronau, Germany). Plants were watered automatically twice a day during cultivation. Measurements were performed using plants 28 or 32 days after sowing.

Isolation of thylakoids and PSII enriched membrane particles

For isolation of spinach thylakoids and PSII-enriched thylakoid membrane particles (BBY particles), fresh spinach leaves were bought from a local supermarket in Szeged, Hungary, and prepared as described in Berthold et al. (1981). For measurements with LIFT and FL3000, the final concentration of thylakoids was adjusted to equivalent chlorophyll *a* concentration of 10 µM (~ 10 µg mL^{-1}).

DCMU and DBMIB treatment

To manipulate the ChlF relaxation kinetics in thylakoid samples, we used 3-(3,4-dichlorophenyl)-1,1-dimethylurea (DCMU) and 2,5-dibromo-5-methyl-6-isopropyl-benzoquinone (DBMIB), which inhibit selectively the reoxidation of Q_A^- in PSII and of PQH_2 at the $cytb_6f$ complex, respectively (Lazár et al. 2001; Kurisu et al. 2003). A thylakoid suspension of 3 mL was transferred to transparent plastic cuvettes. After 5-min dark-adaption, DCMU and DBMIB were added to final concentration of 5 µM (1.17 µg mL^{-1}) and 0.66 µM (0.213 µg mL^{-1}), respectively. Samples were stirred manually and followed by either LIFT or FL3000 measurements using FRR flash for 0.75 ms ($FRRF_{0.75ms}$) or STF, respectively. The number of technical replicates was 3–5. In addition, intact leaves were treated with DCMU to observe ChlF induction curves under conditions of blocked electron transport between Q_A and Q_B. Plants were dark-adapted overnight, then fully expanded leaves were left untreated or were subjected to 200 µM DCMU in 50 mL Milli-Q water (Tóth et al. 2005). The control was left untreated because a control with 1% ethanol in distilled water showed no effect on F_m and little effect on the ChlF rise compared to untreated leaves (Tóth et al. 2005). However, no ethanol was used in the DCMU solution to avoid possible side effects (Haldimann and Tsimilli-Michael 2005). DCMU was grinded to powder in order to dissolve it better in water. In the dark, one leaf per plant was left for 6 h in DCMU solution, then wiped and left for 30 min in the air. Measurements on attached leaves were done using 5 $FRRFs_{0.75ms}$ followed by one MTF for 750 ms (MTF_{750ms}). Only the first of the 5 $FRRFs_{0.75ms}$ is shown in the result section. Measurements were replicated with six different plants.

Anaerobic treatment under nitrogen atmosphere

Oxygen depletion inhibits the plastid terminal oxidase (PTOX), which normally keeps PQ in an oxidized state in the dark (Bohme et al. 1971; Cournac et al. 2000; Feilke et al. 2014). Anoxic treatment was used to manipulate the level of PQ reduction non-invasively in living plants (Tóth et al. 2007b). The anoxic atmosphere was maintained in the LI-COR 6400 transparent 2 × 3 cm chamber head (LI-COR, Inc., Nebraska USA) using nitrogen gas (N_2). Air inflow into the chamber came either from the ambient air (as control, with 400 ppm CO_2) or from N_2 gas supply without oxygen (containing < 1.5 ppm CO_2). The air flow rate during the measurements was 300 µmol air s^{-1}, and the block temperature of the LI-COR was kept at 20 °C. Prior to measurements, plants were dark-adapted overnight. A fully expanded leaf was inserted into the chamber and measured with the LIFT instrument through the transparent front window. Measurements were started after 5-min exposure to control or N_2 atmosphere using 5 $FRRFs_{0.75ms}$ followed by one MTF_{750ms}. After another 5 min, measurements were repeated using 5 FRR flashes for 2.5 ms ($FRRFs_{2.5ms}$). Each first flash of the 5 $FRRFs_{0.75ms}$ and 5 $FRRFs_{2.5ms}$ is shown the result section. Measurements were replicated with six different plants.

Light response curves

To study electron transport kinetics of light-adapted plants, control plants of the N_2 atmosphere experiment were subjected to increasing levels of blue light provided by the LED (445 nm) light source of the LIFT instrument. The size of the illumination spot was around 3 cm^2. A light response measurement consisted of a total of 160 $FRRF_{0.75ms}$ triggered at a 5-s interval. At every light intensity (30, 100, 300, 700 µmol photons m^{-2} s^{-1}), ChlF was monitored over a period of 200 s by applying 40 consecutive $FRRF_{0.75ms}$. Light response curves were replicated with six different plants.

Fluorescence measurements

Different methods have been developed to separate absolute ChlF intensity and background radiation from relative

changes of ChlF yield due to Q_A reduction. This allows comparison of minimal ChlF (F_o in dark-adapted state, and F' in background light) and maximal ChlF (F_m in dark-adapted state, and F_m' in background light) at initial redox state of Q_A and when Q_A is fully reduced at the end of a saturating flash, respectively (Schreiber et al. 1986a; Strasser et al. 1995; Kolber et al. 1998). Two different fluorometers as described below were used in this study. The LIFT method requires no additional saturating light pulse besides the measuring flashlets. Therefore, it is referred to as a modulated method. In contrast, the FL3000 fluorometer uses weak measuring pulses and a strong excitation flash. Therefore, it is referred to as a double-modulated method.

FL3000 measurements

ChlF relaxation after a STF was monitored by weak, non-actinic measuring flashes in increasing time intervals (Trtilek et al. 1997; Vass et al. 1999). These double-modulated ChlF measurements were performed with a FL3000 fluorometer (Photon Systems Instruments Ltd., Brno, Czech Republic) (Trtilek et al. 1997). The instrument is equipped with red LEDs (639 nm) for both actinic (20 µs with an excitation power of 1020 µmol photons m^{-2} s^{-1}) and weak, non-actinic measuring flashes of 8 µs, with a measuring delay of 7 µs. Changes in ChlF yield can be measured in a very broad time range, from 100 µs to 100 s. Within this time range, reoxidation of Q_A^- by both forward and backward reactions can be studied (Vass et al. 1999). The reoxidation phase after the STF usually shows three relaxation phases with corresponding τ_1, τ_2, and τ_3 time constants.

LIFT measurements

The newly developed compact LIFT instrument (Version LIFT-REM, Soliense Inc., New York, USA) is equipped with a blue LED (445 nm) excitation source. Excitation protocols composed of up to 7500 flashlets are used to manipulate the level of photosynthetic activity and ChlF (Fig. 1). ChlF emission is detected at 685 (±10) nm. The LIFT device monitors any background signal in the detector range during inter-flashlet periods and subtracts this signal from the in-flashlet ChlF signal. The ChlF yield is internally normalized against excitation power of each flashlet to correct for smaller fluctuations. Flashlet excitation power along the entire FRR excitation phase is kept at a constant level. This was verified by observing a flat fluorescence transient using a fluorescence standard with constant quantum yield of fluorescence.

All measurements were done from a 0.6 m distance with flashlet length of 1.6 µs. The three used FRR flashes differ in the length of flashlet interval and ChlF induction phase (Table 1). $FRRF_{0.75ms}$ consists of 300 flashlets with a 2.5-µs

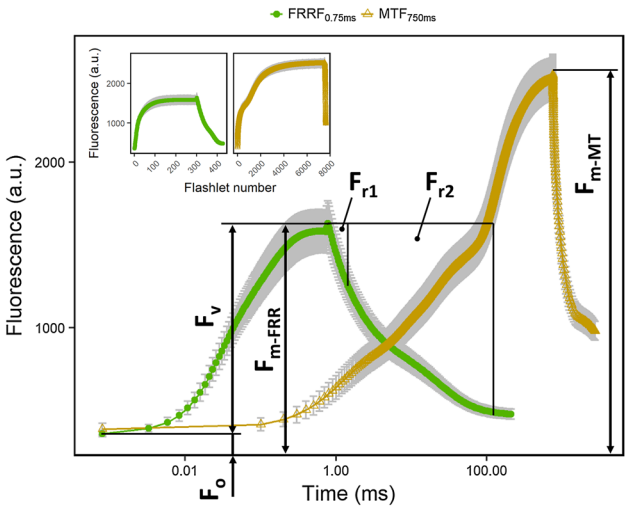

Fig. 1 Chlorophyll fluorescence transients of spinach leaves induced by fast repetition rate flash ($FRRF_{0.75ms}$) and multiple turnover flash (MTF_{750ms}) are presented on a logarithmic time scale. The $FRRF_{0.75ms}$ protocol (green circles) consists of 300 subsaturating flashlets (40,000 µmol photons m^{-2} s^{-1}) in the first 0.75 ms to saturate maximum fluorescence (F_{m-FRR}). Minimum fluorescence (F_o), F_{m-FRR}, and variable fluorescence (F_v) were used for calculation of the quantum efficiency of photosystem II (F_v/F_m) in the dark-adapted state. The excitation flash is followed by 127 flashlets at exponential decreasing repetition rate resulting in chlorophyll fluorescence relaxation. The area above this relaxation curve was restricted by two time period ($r_1 = 0.65$ ms and $r_2 = 120$ ms after F_{m-FRR} was reached) resulting in two relaxation phases (F_{r1} and F_{r2}). The areas were normalized with the corresponding time period and with F_v in order to retrieve the reoxidation efficiency of the primary quinone acceptor (Q_A) in the given relaxation phases (F_{r1}/F_v and F_{r2}/F_v). The MTF_{750ms} (yellow triangles) protocol consists of 7500 subsaturating flashlets (1000 µmol photons m^{-2} s^{-1}) in the first 750 ms and induced the maximum fluorescence (F_{m-MT}). Inset: Chlorophyll fluorescence transients against flashlet number of $FRRF_{0.75ms}$ and MTF_{750ms} are shown. Error bars show standard deviation of the mean ($n = 6$ plants). (Color figure online)

interval summing up to the 0.75 ms induction phase. The ChlF relaxation phase after the $FRRF_{0.75ms}$ consists of 127 flashlets. The interval between those flashlets increases exponentially with

$$j_i = 10^{1.28+0.0215\times i}\,\mu s,$$

where j_i is the interval length of the ith flashlet. For the DCMU and DBMIB experiments, the excitation power was approximately 20,000 µmol photons m^{-2} s^{-1} for the ChlF induction phase using $FRRF_{0.75ms}$. Due to the restricted excitation power of the LEDs, the $FRRF_{0.75ms}$ lasts longer than a proper STF in order to get F_{m-FRR} saturated. For intact plants, the excitation power was 40,000, 24,000, and 1000 µmol photons m^{-2} s^{-1} for the ChlF induction phase using $FRRF_{0.75ms}$, $FRRF_{2.5ms}$, and MTF_{750ms}, respectively. The interval between the flashlets for MTF_{750ms} was extended from 2.5 to 100 µs due to exhausting of LED at

Table 1 Different excitation protocols are shown: Fast repetition rate flash for 0.75 ms ($FRRF_{0.75ms}$) and for 2.5 ms ($FRRF_{2.5ms}$) as well as saturating multiple turnover flash for 750 ms (MTF_{750ms}). In the induction phase, flashlet interval is constant for given amount of flashlets and interval, while it increases exponentially in the relaxation phase to allow reoxidation of the primary quinone acceptor (Q_A). Flashlet length is always 1.6 µs and has in all flashes the same specified excitation power

Excitation protocol	Induction phase (ms)	Number of flashlets in induction phase	Flashlet interval in induction phase (µs)	Relaxation phase (ms)	Number of flashlets in relaxation phase	Flashlet length (µs)
$FRRF_{0.75ms}$	0.75	300	2.5	209	127	1.6
$FRRF_{2.5ms}$	2.5	1000	2.5	209	127	1.6
MTF_{750ms}	750	7500	100	1975	127	1.6

longer flashes. This resulted in the lower excitation power. Excitation power was measured at 1% duty cycle using a 5-s calibration flash measured by a quantum sensor (LI-190R, LI-COR, Inc.) and then extrapolated to 100%. For application of constant actinic light, the intensity of the blue LIFT LED in DC mode was calibrated using a quantum sensor (LI-190R, LI-COR, Inc.) at 0.6-m distance.

Analysis of LIFT and FL3000 raw data

For the calculation of F_v/F_m, the variable ChlF (F_V) is the difference between F_m and F_o. In the LIFT analysis, F_m is represented by F_{m-FRR} as the averaged ChlF yield of 301st–302nd flashlet. F_o is the ChlF yield of the first flashlet (Fig. 1). In the FL3000 analysis, F_m is represented by F_{m-ST} and measured 0.15 ms after the STF. F_o is measured before the STF. The Q_A^- reoxidation efficiency is calculated from the ChlF relaxation kinetics as follows:

$$F_{r1,2}/F_V = \left(F_V \times t_{1,2} - \sum F_i \times j_i\right) \Big/ \left(F_V \times t_{1,2}\right)$$

Here, F_i is the ChlF yield in the relaxation phase at flashlet *i*. F_i is multiplied by j_i and summed up to represent the area of ChlF relaxation up to $t_1 = 0.65$ ms (for F_{r1}) and $t_2 = 120$ ms (for F_{r2}). In case of the FL3000 data, the time points for t_1 and t_2 were 0.52 ms and 100 ms after the STF, respectively, due to different relaxation protocols. The light-adapted states of F_o, F_{m-FRR}, F_v, and $F_{r1,2}$ are denoted as F', F_{m-FRR}', F_q', and $F_{r1,2}'$, respectively.

Statistics

Analysis of variance (ANOVA) was used to calculate significant differences ($p < 0.05$) followed by Tukey's test for pairwise comparison. Due to the small sample size ($n < 7$), normal distribution and homogeneity of variance were assumed. Analysis was done by R program using the *multcomp* package.

Results

Photosynthetic characteristics were studied by measuring light-induced ChlF transients using both the modulated LIFT and the double-modulated FL3000 device with an emphasis on the properties of electron transport from PSII towards PSI.

Determination of F_m levels and electron transport kinetics

We used the $FRRF_{0.75ms}$ and MTF_{750ms} protocol to study the Induction of F_{m-FRR} and F_{m-MT}, respectively (Table 1). The F_{m-FRR} in control leaves was significantly lower than F_{m-MT} (Figs. 1, 2a, b). Under control conditions, F_{m-FRR} saturated earliest at about 0.25 ms depending on the excitation power (Fig. S1). At the end of the induction phase, a small peak of ChlF occurs pointing towards a minor ChlF quenching during the high excitation power of the $FRRF_{0.75ms}$. These spikes contributed to F_{m-FRR} resulting in F_v/F_m values independent of the excitation power. In contrast, F_{m-MT} in intact leaves was reached after 750 ms and showed the same F_{m-MT} as in the presence of DCMU (Fig. 2b).

We studied ChlF relaxation on attached leaves in the dark by using $FRRF_{0.75ms}$ under control and N_2 atmosphere. The absence of O_2 in the latter condition prevents reoxidation of the PQ pool in the dark (Tóth et al. 2007b). After 5 min in the N_2 atmosphere, ChlF relaxation phase was significantly altered compared to control conditions (Fig. 2a). While F_v/F_m did not change under control and N_2 atmosphere, F_{r1}/F_v in the N_2 atmosphere decreased significantly to 0.16 (±0.01) compared to 0.18 (±0.01) in the control (Fig. 3). In contrast, F_{r2}/F_v was significantly increased in the N_2 atmosphere compared to the control. Notably, also the ChlF induction phase of MTF_{750ms} differed in N_2 atmosphere compared to control (Fig. 2b). Following MTF_{750ms}, we kept the plants for additional 5 min under the control or N_2 atmosphere. This allowed S-states of the OEC to relax in the dark (Kolber et al. 1998), whereas the PQ pool remained reduced in the N_2 atmosphere. Then a subsequent measurement using $FRRF_{2.5ms}$ was initiated. F_{m-FRR} in the control

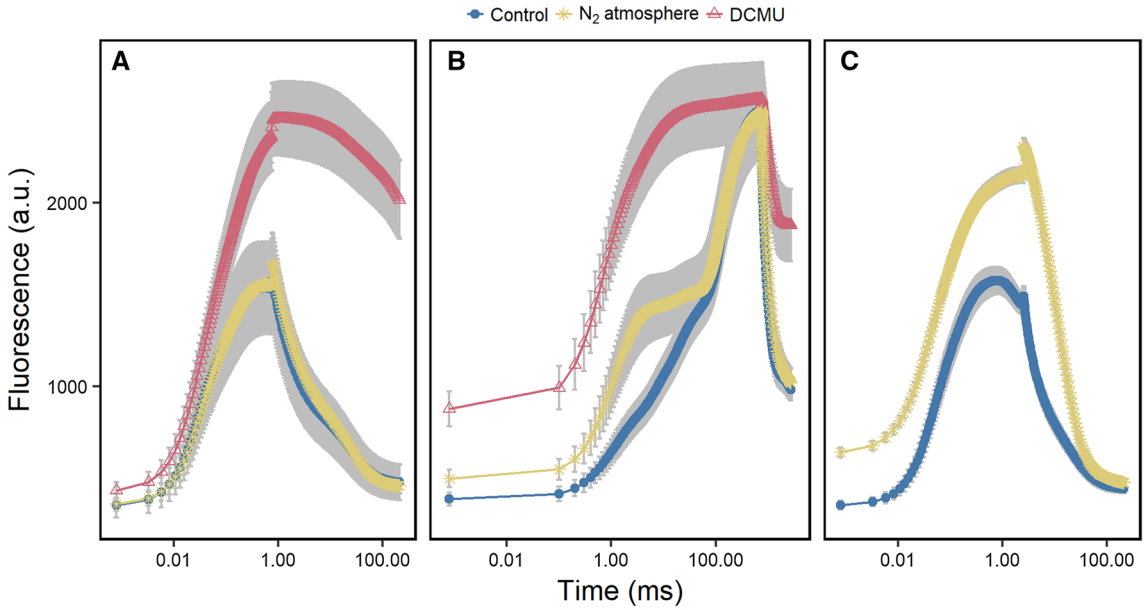

Fig. 2 Dark-adapted spinach leaves were subjected to a 3-(3,4-dichlorophenyl)-1,1-dimethylurea (DCMU) treatment and nitrogen (N_2) atmosphere, which prevent reoxidation of the primary quinone acceptor (Q_A), and plastoquinone (PQ) pool in the dark, respectively. Under those treatments, fast repetition rate flash for 0.75 ms ($FRRF_{0.75ms}$, **a**), multiple turnover flash (MTF_{750ms}, **b**), and fast repetition rate flash for 2.5 ms ($FRRF_{2.5ms}$, **c**) were used to study chlorophyll fluorescence induction and relaxation. $FRRF_{0.75ms}$ was performed after 5 min in control or N_2 atmosphere (for DCMU treatment see "Materials and methods" section). MTF_{750ms} was performed after $FRRF_{0.75ms}$. $FRRF_{2.5ms}$ was performed after additional 5 min in control or N_2 atmosphere. Chlorophyll fluorescence transients are presented on a logarithmic time scale. Error bars showing standard deviation of the mean ($n=6$ plants)

treatment was reached at around 750 µs and then the ChlF signal started to decline (Fig. 2c). In the N_2 atmosphere, the ChlF level continued to increase during the $FRRF_{2.5ms}$ without reaching saturation. This resulted in a significantly increased F_{m-FRR} relative to the control. In addition, F_o levels were higher in the N_2 atmosphere compared to control in the subsequent flashes (Fig. 2b, c). This led to significantly lowered F_v/F_m under N_2 atmosphere using $FRRF_{2.5ms}$ (p value <0.001). In summary, F_{m-MT} induction in untreated leaves using MTF_{750ms} was confirmed by the same F_m induced in DCMU-treated leaves. Full saturation of F_{m-FRR} level was confirmed using $FRRF_{2.5ms}$ under two conditions: (1) plants were in controlled, aerobic conditions (PQ pool was oxidized); and (2) the leaf was fully dark-adapted (OEC mainly in the S_1-state) (Delosme and Joliot 2002). The influence of increased PQ pool reduction was reflected in decreased F_{r1}/F_v, and increased F_o and F_{m-FRR}.

Comparison of electron transport kinetics measured by the LIFT and FL3000 device

We compared the ChlF relaxation kinetics acquired by the modulated LIFT to those of the double-modulated FL3000 device. For that purpose, we treated the thylakoids with different electron transport inhibitors. The two methods resulted in similar ChlF relaxation curves (Fig. 4). The F_v/F_m values calculated from the LIFT measurements ranged between 0.58 (±0.01) for BBY and 0.7 (±0.02) for thylakoids (Fig. 5a). The FL3000 device showed generally lower F_v/F_m values: 0.31 (±0.04) for BBY particles and 0.49 (±0.02) for thylakoids (Fig. 5b). In BBY particles, electron transport is impaired after the Q_B site since the PQ pool is partly, and the PSI fully removed (Berthold et al. 1981). DBMIB binds to the $cytb_6f$ complex, which blocks the reoxidation of the PQ pool (Bohme et al. 1971). Consequently, BBYs and DBMIB-treated thylakoids showed slower ChlF relaxation kinetics compared to thylakoids, resulting in significantly lower F_{r1}/F_v and F_{r2}/F_v values in both methods (Fig. 5c–f). F_{r1}/F_v for the LIFT device ranged from 0.21 (±0.008) for thylakoids to 0.04 (±0.008) for BBY (Fig. 5c). The F_{r1}/F_v values calculated from the FL3000 measurements were in general higher (e.g., 0.34 (±0.025) for thylakoids and 0.1 (±0.013) for BBY, Fig. 5d) but showed the same tendency as in the LIFT measurements. F_{r2}/F_v showed increasing difference between the control and treated samples reflecting impaired electron transport (Fig. 5e, f). In summary, F_{r1}/F_v and F_{r2}/F_v measured with both devices responded specifically to the treatments which block electron transport at different steps.

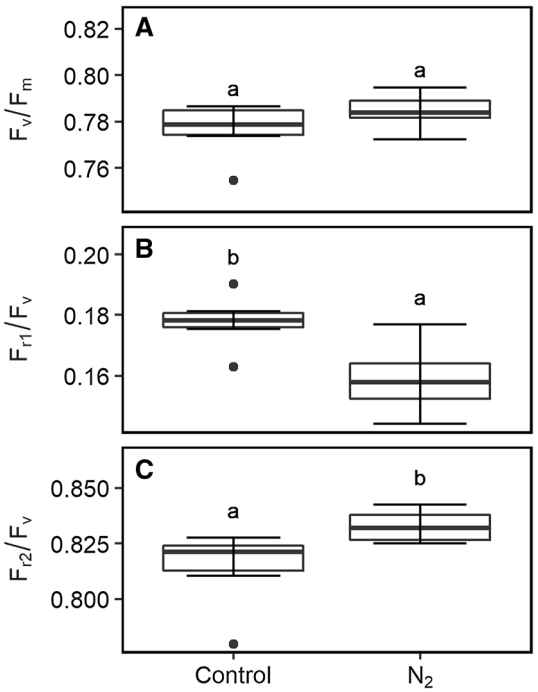

Fig. 3 Boxplot of quantum efficiency of the photosystem II (F_v/F_m, **a**), efficiency of primary quinone acceptor (Q_A) reoxidation in 0.65 ms (F_{r1}/F_v, **b**), and 120 ms (F_{r2}/F_v, **c**) relaxation phases of dark-adapted attached spinach leaves are shown. Measurements took place 5 min after exposure to control or nitrogen (N_2) atmosphere. Parameters were obtained using fast repetition rate flash ($FRRF_{0.75ms}$) of the light-induced fluorescence transient (LIFT) instrument. Box represents inter-quartile range, bold horizontal bar the median, the discontinuous lines the upper and lower quartile, and outlier data points (> 1.5 × inter-quartile range) are depicted by a point ($n = 6$ plants). Boxes labeled with different letters differ significantly from each other according to Tukey's multiple comparisons of means

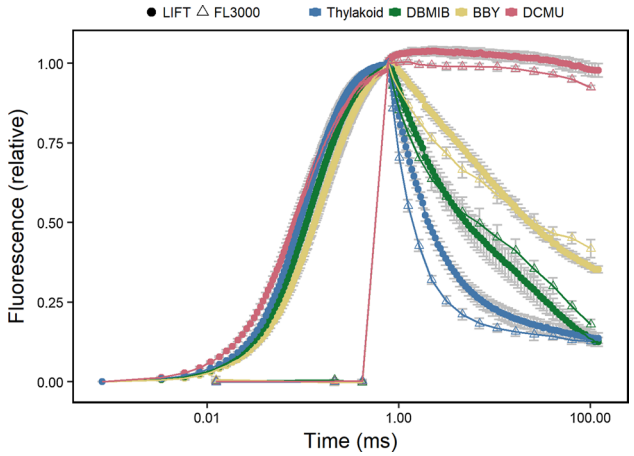

Fig. 4 Chlorophyll fluorescence transients of isolated spinach thylakoids and photosystem II particles (BBY) are presented on a logarithmic time scale. The measurements were performed either by the light-induced fluorescence transient (LIFT) device (closed circles) or with the double-modulated FL3000 fluorometer (open triangles). Thylakoid samples (10 µg chlorophyll/mL) were either untreated, or treated with 5 µM 3−(3,4-dichlorophenyl)-1,1-dimethylurea (DCMU) or 0.66 µM 2,5-dibromo-5-methyl-6-isopropyl-benzoquinone (DBMIB). Chlorophyll fluorescence signals are double normalized so that the signal starts from 0 for measured minimum fluorescence (F_o), and has a total amplitude of 1. Chemicals were added in the dark and samples were dark-adapted for 3 min before measurement. Error bars show standard deviation ($n = 5$, except DCMU FL3000 and DBMIB FL3000 $n = 3$)

Electron transport kinetics measured under ambient light

We measured light-response curves on attached spinach leaves in order to follow the light saturation of electron transport rate. F′ initially increased with increasing light intensities, but this increase was then reversed, most likely due to NPQ formation (Fig. 6a). Simultaneously, F_{m-FRR}' decreased in response to increasing light intensities due to NPQ formation. F_{m-FRR}' showed smaller absolute differences than F_{m-MT}' compared to the corresponding dark-adapted states (Fig. 6b).

The F_q'/F_m' values we obtained with the $FRRF_{0.75ms}$ protocol correlated highly with F_q'/F_m' values we retrieved with the MTF_{750ms} protocol ($r^2 = 0.99$) during the measurements of blue-light response curves (Fig. 7). This demonstrates that $FRRF_{0.75ms}$ and MTF_{750ms} measurements result in basically the same parameters with the exception of an offset, at least under these standard conditions. Increasing light intensities resulted in a significant decrease in the F_q'/F_m' (Fig. 8a). In contrast, F_{r1}'/F_q' and F_{r2}'/F_q' were less affected by the higher light intensities (Fig. 8b, c). Upon dark to light transition at 30 µmol photons m^{-2} s^{-1}, F_{r1}'/F_q' decreased from 0.18 (±0.009) to 0.10 (±0.023) and increased to 0.2 (±0.01) at the last two light intensities. F_{r2}'/F_q' increased from 0.81 (±0.018) to 0.95 (±0.035) and then was stabilized at 0.89 (±0.02) at the higher light intensities. F_{r1}'/F_q' measured in the light was not significantly different from dark-adapted values, with the exception of the initial light step at 30 µmol photons m^{-2} s^{-1}. In summary, ChlF relaxation kinetics in the light were little affected by increasing light intensities and NPQ, whereas F_q'/F_m' decreased.

Discussion

We induced ChlF transients by using different LIFT-FRR excitation protocols ($FRRF_{0.75ms}$ and MTF_{750ms}) at 0.6 m distance (Fig. 1). F_v/F_m and F_q'/F_m' were highly correlated between the two protocols (Fig. 7). Furthermore, we characterized a range of photo-physiological properties with an emphasis on the kinetics of electron transport from PSII towards PSI. These kinetics are determined by the well-established architecture of photosynthetic linear electron transport chain and can be observed via ChlF relaxation

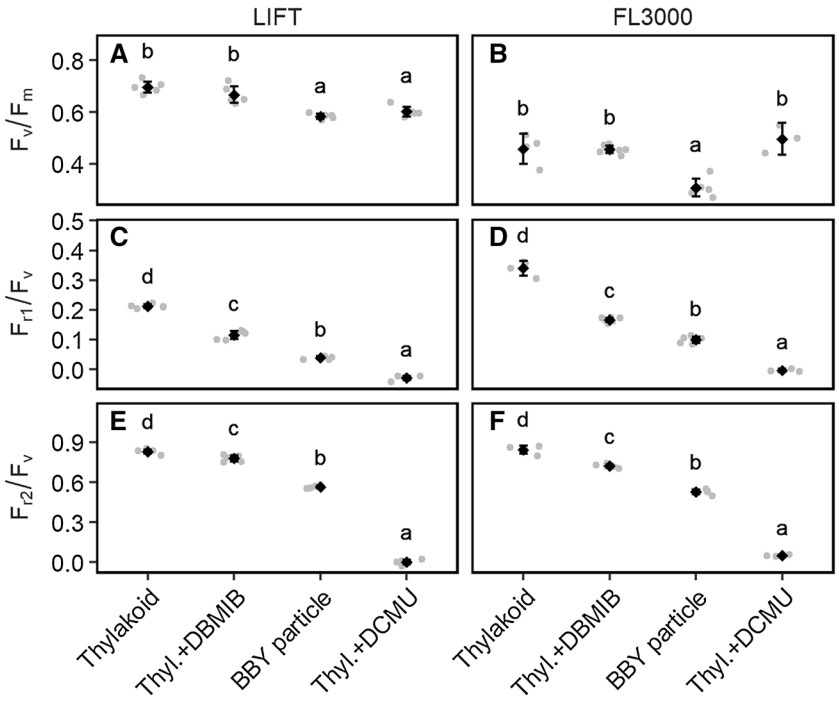

Fig. 5 Comparison of photosystem II quantum efficiency (F_v/F_m, **a, b**) and efficiency of primary quinone acceptor (Q_A) reoxidation in 0.65 ms (F_{r1}/F_v, **c, d**), and 120 ms (F_{r2}/F_v, **e, f**) relaxation phases in dark-adapted state acquired by light-induced fluorescence transient (LIFT) and double-modulated FL3000 fluorometer. Measurements were carried out on isolated spinach thylakoids and BBY particles. Thylakoid samples (10 µg chlorophyll/mL) were either untreated or treated with 5 µM 3−(3,4-dichlorophenyl)-1,1-dimethylurea (DCMU) or 0.66 µM 2,5-dibromo-5-methyl-6-isopropyl-benzoquinone (DBMIB), resulting in different chlorophyll fluorescence relaxations as shown in Fig. 4. Black diamonds show mean values and error bars indicate the 95% confidence intervals. Individual data points are depicted by a grey point ($n=5$, except DCMU FL3000 and DBMIB FL3000 $n=3$). Means labeled with different letters differ significantly from each other according to Tukey's multiple comparisons of means

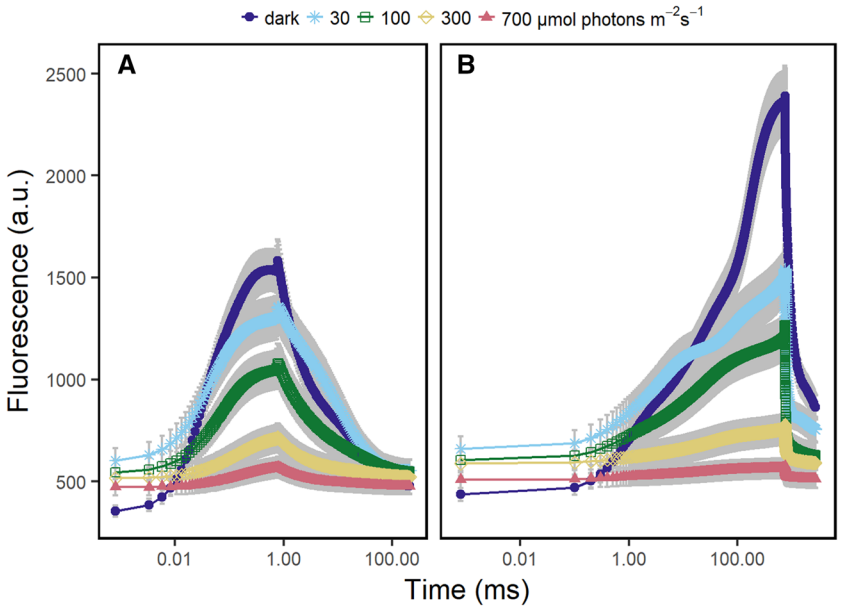

Fig. 6 Chlorophyll fluorescence response of attached spinach leaves measured under different intensities of background irradiance by the light-induced fluorescence transient (LIFT) instrument. Leaves were exposed to 0 (dark-adapted), 30, 100, 300, and 700 µmol photons m^{-2} s^{-1} blue light (445 nm). Fast repetition rate flash ($FRRF_{0.75ms}$, **a**) and multiple turnover flash (MTF_{750ms}; **b**) were performed on dark-adapted samples and after reaching the steady state at each light intensity (after 3 min). Chlorophyll fluorescence transients are presented on a logarithmic time scale. Error bars show the standard error of the mean ($n=6$ plants)

reflecting the kinetics of Q_A^- reoxidation (Vass et al. 1999). Efficiency of Q_A^- reoxidation was assessed in 0.65 ms and 120 ms relaxation phases after the FRR excitation, expressed in the F_{r1}/F_v and F_{r2}/F_v parameter, respectively. These simple parameters reflect the overall reoxidation of Q_A^- during the indicated time periods. In the light, F_{r2}'/F reflected

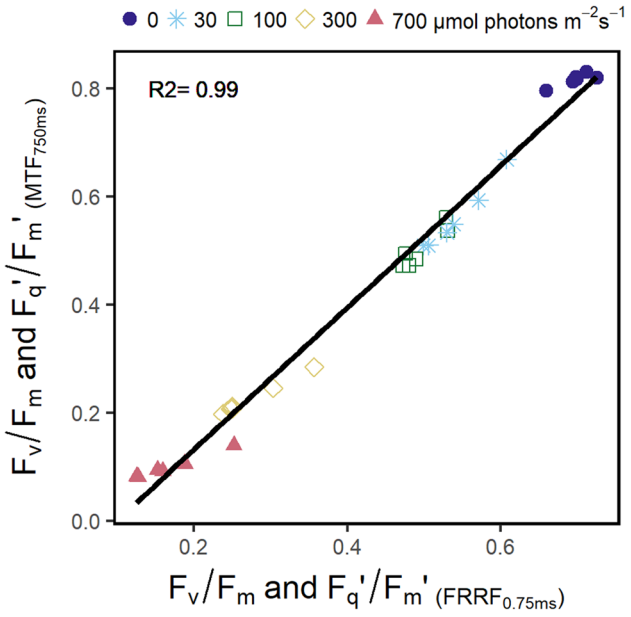

Fig. 7 Correlation of quantum efficiency of the photosystem II in the dark-adapted state (F_v/F_m) and the light-adapted state (F_q'/F_m') obtained by fast repetition rate flash ($FRRF_{0.75ms}$) and multiple turnover flash (MTF_{750ms}) during a blue-light response curve of spinach leaves. Maximum fluorescence (F_m in the dark and F_m' in the light) represents chlorophyll fluorescence yield of the averaged 300th and 301st flashlet of the $FRRF_{0.75ms}$ respective the yield of the 7500th flashlet in case of the MTF_{750ms}. Variable fluorescence (F_v in the dark or F_q' in the light) is the difference between F_m or F_m' and the chlorophyll fluorescence yield of the first flashlet (F_o in the dark or F' in the light). The regression formula was $y = -0.13 + 1.31 \times x$. Measurements were performed using the light-induced fluorescence transient (LIFT) device ($n = 6$ plants)

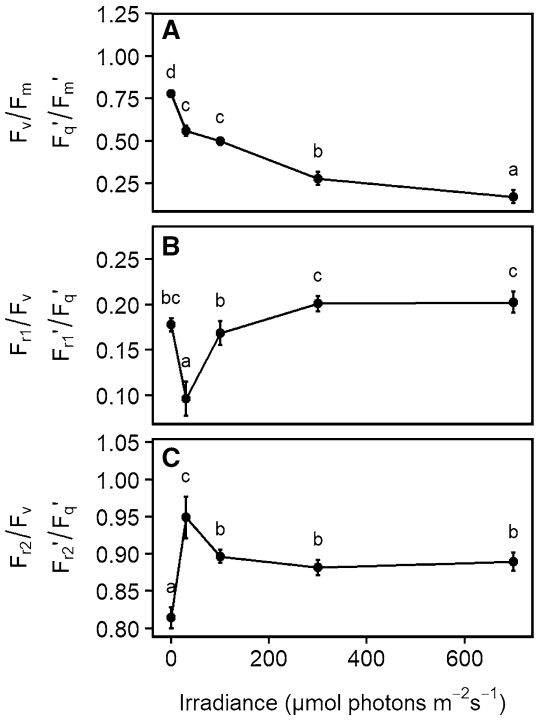

Fig. 8 Quantum efficiency of the photosystem II (F_v/F_m in the dark, and F_q'/F_m' in the light, **a**) and efficiency of primary quinone acceptor (Q_A) reoxidation in 0.65 ms (F_{r1}/F_v in the dark, and F_{r1}'/F_q' in the light, **b**,) and 120 ms (F_{r2}/F_v in the dark, and F_{r2}'/F_q' in the light, **c**) relaxation phases of attached spinach leaves were measured under different intensities of background irradiance. Parameters were acquired using fast repetition rate flash ($FRRF_{0.75ms}$) of the light-induced fluorescence transient (LIFT) instrument. Black dots show mean values and error bars indicate the 95% confident interval ($n = 6$ plants). Means labeled with different letters differ significantly from each other according to Tukey's multiple comparisons of means

electron transport capacity from Q_A towards PSI and was far less sensitive to increasing light intensities than F'/F_m' (Fig. 8). The results provide additional information about electron transport, which are not reflected by the F_v/F_m parameter.

Maximum fluorescence

We demonstrated ChlF induction at 0.6 m distance by using the LIFT instrument on attached spinach leaves. F_{m-MT} in the control leaves was reached at 750 ms after multiple turnover of PSII reaction centers (Fig. 2b). That F_{m-MT} was indeed saturated by using MTF_{750ms}, was confirmed by using the DCMU treatment, which showed the same ChlF level. DCMU inhibits Q_A^- reoxidation and induces F_{m-MT} in intact leaves (Tóth et al. 2005). In contrast to F_{m-MT}, F_{m-ST} is reached within 40 to 60 µs within one full turnover of the PSII reaction centers (Kolber et al. 1998; Nedbal et al. 1999; Belyaeva et al. 2014). The level of F_{m-ST} is about 50% lower compared to F_{m-MT} and is based on fully reduced Q_A (e.g., Samson and Bruce 1996; Schansker et al. 2014). The difference between F_{-MT} and F_{m-ST} is suggested to be caused by additional ChlF quenchers that are removed during multiple turnovers (Delosme 1967; Kalaji et al. 2017). In this study, the F_{m-FRR} induced by $FRRF_{0.75ms}$ saturated at about 0.25 ms at highest excitation power of 40,000 µmol photons m^{-2} s^{-1} (Fig. S1). Within this time range, the OEC is already in the second turnover and Q_A^- is once reoxidized by Q_B (Ananyev and Dismukes 2005b; Pérez-Navarro et al. 2016). The reoxidation of Q_A^- by Q_B and Q_B^- has time constants of 0.2 ms and 0.7 ms, respectively (Bowes and Crofts 1980; de Wijn and van Gorkom 2001; Tomek et al. 2001). The second time constants may vary with respect to the kinetics of H^+ uptake by Q_B^- (Petrouleas and Crofts 2005). The saturating behavior of F_{m-FRR} strongly indicates that photochemical processes stabilized within the $FRRF_{0.75ms}$ (Fig. S1). In agreement, the derived F_v/F_m values were independent from the used excitation power. We conclude that F_{m-FRR} reflected fully reduced Q_A mainly associated with Q_B^-.

Using the $FRRF_{2.5ms}$ protocol, F_{m-FRR} declined after reaching a plateau under control conditions (Fig. 2c). This behavior was only observed when the PQ pool was oxidized and the sample was dark-adapted. Similarly, the polyphasic ChlF rise during a MTF of 15,000 µmol photons m^{-2} s^{-1} records a local ChlF maximum at about 2 ms (J-step) (Schreiber 1986a; Tóth et al. 2007a; Schansker et al. 2011). This ChlF peak appears only when the sample is in the S_1-state, i.e., dark-adapted (Strasser 1997). In the ChlF decline, Q_A reduction is overcome by Q_A^- reoxidation via the oxidized PSII primary donor ($P680^+$), which accumulates during the slow S_3–S_4 transition of the OEC (Schansker et al. 2011; Kalaji et al. 2017). The phase of ChlF decline matches time wise with the formation of Q_B^{2-} (Bowes and Crofts 1980; de Wijn and van Gorkom 2001). After 2 ms, electron delivery of the OEC proceeds and re-reduction of Q_A, further accumulation of Q_B^{2-} and exchange of Q_B^{2-} by an oxidized PQ takes place (Petrouleas and Crofts 2005). These processes lead to an increasing ChlF signal during a MTF, known as thermal phase (Delosme 1967; Lazár 2006). It was shown before that PQ pool reduction leads to a higher ChlF signal by releasing non-photochemically quenched ChlF (Vernotte et al. 1979; Haldimann and Tsimilli-Michael 2005). In agreement, F_{m-FRR} increased without reaching saturation when the PQ pool was already reduced in the dark (Fig. 2c). Similarly, F_o under N_2 atmosphere was also higher than in the control but was the same in the subsequent $FRRF_{2.5ms}$ (p value = 0.403, data not shown) due to reoxidation of PQ pool during the flash. F_o yield was shown to be dependent on PQ redox state and can be recovered by far-red light pulse (Diner 1977; Hohmann-Marriott et al. 2010; Kalaji et al. 2017). However, this additional ChlF quenching is probably not directly controlled by the PQ pool (Tóth et al. 2005). It may be induced by the occupancy of the Q_B-pocket or by conformational changes in the PSII complex (Falkowski et al. 2004; Schansker et al. 2014; Magyar et al. 2018; Prášil et al. 2018). This might explain that F_{m-ST} (when only Q_A is reduced) cannot surpass the ChlF level at the J-step (Schreiber 1986a). Another reason for the lower F_{m-ST} compared to the J-step might be that STF induced a quenching mechanism during the reduction phase of Q_A. At the end of the $FRRF_{0.75ms}$ induction phase, when changing from fast to low repetition rate flashlets, we noticed an instantaneous ChlF spike (Fig. S1). This indicates a fast-relaxing quenching mechanism. It was suggested earlier that carotenoid triplets quench ChlF within µs when operating with flashes at high excitation power (Schödel et al. 1999; Steffen et al. 2001; Braslavsky and Holzwarth 2012; Belyaeva et al. 2014). In summary, saturated F_{m-FRR} differs from F_{m-ST} in the reduction of Q_B to Q_B^- while Q_A is fully re-reduced. F_{m-FRR} and F_{m-ST} are expected to be comparable since Q_B^- is not known to quench any ChlF (Schansker et al. 2011). The saturation of F_{m-FRR} after 0.25 ms indicates that Q_B^{2-} was not formed. The F_{m-FRR} differs from the J-step in the redox state of the OEC and the accumulation of Q_B^{2-} which influence ChlF (see also Osmond et al. 2017). When reaching F_{m-MT}, at least one additional quencher is removed increasing ChlF signal by a still unclear mechanism (Magyar et al. 2018; Prášil et al. 2018).

Validation of electron transport kinetics

Anaerobiosis inhibits PQ pool reoxidation in the dark (Bohme et al. 1971; Cournac et al. 2000; Feilke et al. 2014). As expected, reduced PQ pool under N_2 atmosphere affected ChlF relaxation and decreased F_{r1}/F_v compared to control (Fig. 3b). ChlF relaxation was compared between the modulated LIFT-FRR and the double-modulated FL3000 device. The two devices measured similar qualitative responses comparable to earlier studies (Deák et al. 2014). However, Q_A^- reoxidation was faster in the first milliseconds when measuring with the double-modulated FL3000 than the LIFT device (Fig. 4). This might be due to the shorter duration of the STF than $FRRF_{0.75ms}$, where the latter reduced Q_B already. In addition, the FRR flashlets have an actinic effect, which partially reduce Q_A and slow down the Q_A^- reoxidation kinetics. The STF of the FL3000 device with 1000 µmol photons m^{-2} s^{-1} was probably not saturating resulting in the lower F_v/F_m values compared to the values derived by the LIFT device. In summary, a wide range of impaired electron transport processes were detected using the ChlF relaxation parameters F_{r1}/F_v and F_{r2}/F_v derived either by the LIFT or the FL3000 device.

Measurements in the light and effect on electron transport kinetics

In the dark, the F_{m-FRR} yield was linked to PQ redox state and S-state of the OEC. The situation is different in the light because NPQ occurs and S-states are randomized. F_{m-FRR}' was interpreted as equilibrium of Q_A reduction, NPQ and subsequent Q_A^- reoxidation (Fig. 6a, Osmond et al. 2017). Accordingly, F_{m-MT}' in the light does not reach saturation because NPQ limits light harvesting and electron transport quenches ChlF very efficiently (Loriaux et al. 2013). The MTF_{750ms} with rather low excitation power (1000 µmol photons m^{-2} s^{-1}) limited F_{m-MT}' saturation additionally. However, F_q'/F_m' derived by $FRRF_{0.75ms}$ during the measurement of blue-light response curve correlated highly with F_q'/F_m' derived by MTF_{750ms} ($R^2 = 0.99$) (Fig. 7). Correspondingly, F_q'/F_m' derived with a previous LIFT device using FRR flashes was shown to be well-correlated to the values measured by a PAM device ($R^2 = 0.89$) (Pieruschka et al. 2010, 2014). Comparable results were also shown by Samson et al. (1999) who carried out a similar experiment using STF and MTF. Dark-light transition at 30 µmol photons m^{-2} s^{-1}

was clearly separated based on the transient shape and the derived F_{r1}'/F_q' and F_{r2}'/F_q' values (Fig. 8). The strong initial response upon illumination appears to represent transition from the dark-adapted state of inactive electron transport to a light-stimulated state of engaged electron transport, e.g., activation of RUBISCO in the first few minutes of light acclimation (Kono and Terashima 2014). In conclusion, F_q'/F_m' derived by $FRRF_{0.75ms}$ approximate F_q'/F_m' values derived by STF or MTF.

The F_{m-ST} and F_{m-MT} signal, along with F_v/F_m and NPQ, are the most common photosynthetic parameters used in ChlF-assisted plant phenomics (Furbank and Tester 2011). These properties are relatively easy to measure by using existing ChlF techniques, and they are extremely sensitive to a range of photo-physiological properties of plants. At the same time, the F_m responses are rather non-specific, requiring additional information to identify the affected photosynthetic mechanisms (Kalaji et al. 2014). In addition, their direct responses to irradiance levels require that these parameters are measured under well-defined light conditions (generally in the dark, with pre-defined periods of dark adaptation), limiting their applications as reporters of physiological conditions under highly variable, natural light conditions. However, the properties of the photosynthetic electron transport from Q_A towards PSI (expressed as F_{r2}'/F_q') remain well-constrained under different ambient light intensities (Fig. 8c). The possibility for automation and measurements in the light using the LIFT method will make it possible to monitor the dynamics of photosynthetic traits under natural conditions.

Conclusion

Simultaneous measurements of F_v/F_m (respective F_q'/F_m') and the kinetics of electron transport between PSII towards PSI expressed as $F_{r1,2}/F_v$ (respective $F_{r1,2}'/F_q'$) parameter provided more detailed information about the photosynthetic apparatus detecting differences in a wide range of physiological conditions. Performing these measurements non-invasively with high time resolution under natural environmental conditions has the potential to improve the efficacy of the photosynthetic phenotyping, while contributing to the advancement of knowledge about photosynthesis and its regulation.

Acknowledgements We would like to thank Angelina Steier for LIFT instrument maintenance. Beate Uhlig, Katharina Wolter-Heinen and Christian Jungmann are acknowledged for greenhouse management and for ensuring optimal plant growth conditions.

Funding This study was performed within the German Plant Phenotyping Network (DPPN) which is founded by the German Federal Ministry for Education and Research (BMBF). Project Identification Number is BMBF 031A053. The work was partly supported (I.V. and A.u.R.) by the Hungarian Ministry for National Economy (Grant No. GINOP-2.3.2-15-2016-00037).

Compliance with ethical standards

Conflict of interest The authors declare that they have no conflict of interest.

References

Ananyev G, Dismukes GC (2005b) How fast can Photosystem II split water? Kinetic performance at high and low frequencies. Photosynth Res 84:355–365. https://doi.org/10.1007/s11120-004-7081-1

Ananyev G, Kolber ZS, Klimov D et al (2005a) Remote sensing of heterogeneity in photosynthetic efficiency, electron transport and dissipation of excess light in *Populus deltoides* stands under ambient and elevated CO_2 concentrations, and in a tropical forest canopy, using a new laser-induced fluorescence transient device. Glob Change Biol 11:1195–1206. https://doi.org/10.1111/j.1365-2486.2005.00988.x

Baker NR (2008) Chlorophyll fluorescence: a probe of photosynthesis in vivo. Annu Rev Plant Biol 59:89–113. https://doi.org/10.1146/annurev.arplant.59.032607.092759

Belyaeva NE, Schmitt FJ, Paschenko VZ et al (2014) Model based analysis of transient fluorescence yield induced by actinic laser flashes in spinach leaves and cells of green alga *Chlorella pyrenoidosa* Chick. Plant Physiol Biochem 77:49–59. https://doi.org/10.1016/j.plaphy.2014.01.017

Berthold DA, Babcock GT, Yocum CF (1981) A highly resolved, oxygen-evolving photosystem II preparation from spinach thylakoid membranes: EPR and electron-transport properties. FEBS Lett 134:231–234. https://doi.org/10.1016/0014-5793(81)80608-4

Bohme H, Reimer S, Trebst A (1971) The effect of dibromothymoquinone, an antagonist of plastoquinone, on non cyclic and cyclic electron flow systems in isolated chloroplasts. Z Naturforschung Part B-Chem Biochem Biophys Biol Verwandten Geb B 26:341–341+

Bowes JM, Crofts AR (1980) Binary oscillations in the rate of reoxidation of the primary acceptor of photosystem II. Biochim Biophys Acta BBA—Bioenerg 590:373–384. https://doi.org/10.1016/0005-2728(80)90208-X

Braslavsky SE, Holzwarth AR (2012) Role of carotenoids in photosystem II (PSII) reaction centers. Int J Thermophys 33:2021–2025. https://doi.org/10.1007/s10765-012-1274-1

Butler WL (1978) Energy distribution in the photochemical apparatus of photosynthesis. Annu Rev Plant Physiol 29:345–378

Cournac L, Redding K, Ravenel J et al (2000) Electron flow between photosystem II and oxygen in chloroplasts of photosystem. J Biol Chem 275:17256–17262. https://doi.org/10.1074/jbc.M908732199

de Wijn R, van Gorkom HJ (2001) Kinetics of electron transfer from QA to QB in photosystem II. Biochemistry 40:11912–11922. https://doi.org/10.1021/bi010852r

Deák Z, Sass L, Kiss É, Vass I (2014) Characterization of wave phenomena in the relaxation of flash-induced chlorophyll fluorescence yield in cyanobacteria. Biochim Biophys Acta BBA—Bioenerg 1837:1522–1532. https://doi.org/10.1016/j.bbabio.2014.01.003

Delosme R (1967) Étude de l'induction de fluorescence des algues vertes et des chloroplastes au début d'une illumination intense. Biochim Biophys Acta BBA—Bioenerg 143:108–128. https://doi.org/10.1016/0005-2728(67)90115-6

Delosme R, Joliot P (2002) Period four oscillations in chlorophyll a fluorescence. Photosynth Res 73:165–168. https://doi.org/10.1023/A:1020430610627

Diner BA (1977) Dependence of the deactivation reactions of Photosystem II on the redox state of plastoquinone pool a varied under anaerobic conditions. Equilibria on the acceptor side of Photosystem II. Biochim Biophys Acta BBA—Bioenerg 460:247–258. https://doi.org/10.1016/0005-2728(77)90211-0

Eshaghi S, Turcsányi E, Vass I et al (2000) Functional characterization of the PS II–LHC II supercomplex isolated by a direct method from spinach thylakoid membranes. Photosynth Res 64:179–187. https://doi.org/10.1023/A:1006404302573

Falkowski PG, Koblfzek M, Gorbunov M, Kolber Z (2004) Development and application of variable chlorophyll fluorescence techniques in marine ecosystems. In: Papageorgiou GC, Govindjee (eds) Chlorophyll a fluorescence: a signature of photosynthesis. Springer Netherlands, Dordrecht, pp 757–778

Feilke K, Yu Q, Beyer P et al (2014) In vitro analysis of the plastid terminal oxidase in photosynthetic electron transport. Biochim Biophys Acta BBA—Bioenerg 1837:1684–1690. https://doi.org/10.1016/j.bbabio.2014.07.016

Fiorani F, Schurr U (2013) Future scenarios for plant phenotyping. Annu Rev Plant Biol 64:267–291. https://doi.org/10.1146/annurev-arplant-050312-120137

Furbank RT, Tester M (2011) Phenomics—technologies to relieve the phenotyping bottleneck. Trends Plant Sci 16:635–644. https://doi.org/10.1016/j.tplants.2011.09.005

Haldimann P, Tsimilli-Michael M (2005) Non-photochemical quenching of chlorophyll a fluorescence by oxidised plastoquinone: new evidences based on modulation of the redox state of the endogenous plastoquinone pool in broken spinach chloroplasts. Biochim Biophys Acta BBA—Bioenerg 1706:239–249. https://doi.org/10.1016/j.bbabio.2004.11.005

Hohmann-Marriott MF, Takizawa K, Eaton-Rye JJ et al (2010) The redox state of the plastoquinone pool directly modulates minimum chlorophyll fluorescence yield in *Chlamydomonas reinhardtii*. FEBS Lett 584:1021–1026. https://doi.org/10.1016/j.febslet.2010.01.052

Kalaji H, Schansker G, Ladle R et al (2014) Frequently asked questions about in vivo chlorophyll fluorescence: practical issues. Photosynth Res 122:121–158. https://doi.org/10.1007/s11120-014-0024-6

Kalaji HM, Schansker G, Brestic M et al (2017) Frequently asked questions about chlorophyll fluorescence, the sequel. Photosynth Res 132:13–66. https://doi.org/10.1007/s11120-016-0318-y

Kautsky H, Hirsch A (1931) Neue Versuche zur Kohlensäureassimilation. Naturwissenschaften 19:964–964. https://doi.org/10.1007/BF01516164

Kolber ZS, Prasil O, Falkowski PG (1998) Measurements of variable chlorophyll fluorescence using fast repetition rate techniques: defining methodology and experimental protocols. Biochim Biophys Acta BBA—Bioenerg 1367:88–106. https://doi.org/10.1016/s0005-2728(98)00135-2

Kono M, Terashima I (2014) Long-term and short-term responses of the photosynthetic electron transport to fluctuating light. J Photochem Photobiol B 137:89–99. https://doi.org/10.1016/j.jphotobiol.2014.02.016

Kurisu G, Zhang HM, Smith JL, Cramer WA (2003) Structure of the cytochrome b(6)f complex of oxygenic photosynthesis: tuning the cavity. Science 302:1009–1014. https://doi.org/10.1126/science.1090165

Lazár D (2006) The polyphasic chlorophyll a fluorescence rise measured under high intensity of exciting light. Funct Plant Biol 33:9–30. https://doi.org/10.1071/FP05095

Lazár D (2013) Simulations show that a small part of variable chlorophyll a fluorescence originates in photosystem I and contributes to overall fluorescence rise. J Theor Biol 335:249–264. https://doi.org/10.1016/j.jtbi.2013.06.028

Lazár D, Tomek P, Ilik P, Naus J (2001) Determination of the antenna heterogeneity of photosystem II by direct simultaneous fitting of several fluorescence rise curves measured with DCMU at different light intensities. Photosynth Res 68:247–257. https://doi.org/10.1023/A:1012973402023

Loriaux SD, Avenson TJ, Welles JM et al (2013) Closing in on maximum yield of chlorophyll fluorescence using a single multiphase flash of sub-saturating intensity. Plant Cell Environ 36:1755–1770. https://doi.org/10.1111/pce.12115

Magyar M, Sipka G, Kovács L et al (2018) Rate-limiting steps in the dark-to-light transition of photosystem II—revealed by chlorophyll-a fluorescence induction. Sci Rep 8:2755. https://doi.org/10.1038/s41598-018-21195-2

Malkin S, Kok B (1966) Fluorescence induction studies in isolated chloroplasts I. Number of components involved in the reaction and quantum yields. Biochim Biophys Acta BBA—Biophys Photosynth 126:413–432. https://doi.org/10.1016/0926-6585(66)90001-X

Müh F, Glöckner C, Hellmich J, Zouni A (2012) Light-induced quinone reduction in photosystem II. Photosyst II 1817:44–65. https://doi.org/10.1016/j.bbabio.2011.05.021

Nedbal L, Trtílek M, Kaftan D (1999) Flash fluorescence induction: a novel method to study regulation of photosystem II. J Photochem Photobiol B 48:154–157. https://doi.org/10.1016/S1011-1344(99)00032-9

Ögren E, Baker NR (1985) Evaluation of a technique for the measurement of chlorophyll fluorescence from leaves exposed to continuous white light. Plant Cell Environ 8:539–547. https://doi.org/10.1111/j.1365-3040.1985.tb01691.x

Osmond B, Chow WS, Wyber R et al (2017) Relative functional and optical absorption cross sections of PSII and other photosynthetic parameters monitored in situ, at a distance with a time resolution of a few seconds, using a prototype light induced fluorescence transient (LIFT) device. Funct Plant Biol. https://doi.org/10.1071/FP17024

Oxborough K, Moore CM, Suggett DJ et al (2012) Direct estimation of functional PSII reaction center concentration and PSII electron flux on a volume basis: a new approach to the analysis of fast repetition rate fluorometry (FRRf) data. Limnol Oceanogr-Methods 10:142–154. https://doi.org/10.4319/lom.2012.10.142

Pérez-Navarro M, Neese F, Lubitz W et al (2016) Recent developments in biological water oxidation. Biocatal Biotransform Bioinorg Chem 31:113–119. https://doi.org/10.1016/j.cbpa.2016.02.007

Petrouleas V, Crofts A (2005) The iron-quinone acceptor complex. In: Wydrzynski T, Satoh K, Freeman J (eds) Photosystem II. Springer, Dordrecht, pp 177–206

Pieruschka R, Klimov D, Kolber ZS, Berry JA (2010) Monitoring of cold and light stress impact on photosynthesis by using the laser induced fluorescence transient (LIFT) approach. Funct Plant Biol 37:395–402. https://doi.org/10.1071/fp09266

Pieruschka R, Albrecht H, Muller O et al (2014) Daily and seasonal dynamics of remotely sensed photosynthetic efficiency in tree canopies. Tree Physiol 34:674–685. https://doi.org/10.1093/treephys/tpu035

Prášil O, Kolber ZS, Falkowski PG (2018) Control of the maximal chlorophyll fluorescence yield by the QB binding site. Photosynthetica. https://doi.org/10.1007/s11099-018-0768-x

Raesch A, Muller O, Pieruschka R, Rascher U (2014) Field Observations with laser-induced fluorescence transient (LIFT) method in barley and sugar beet. Agriculture 4:159–169

Rascher U, Nedbal L (2006) Dynamics of photosynthesis in fluctuating light—commentary. Curr Opin Plant Biol 9:671–678. https://doi.org/10.1016/j.pbi.2006.09.012

Robinson HH, Crofts AR (1983) Kinetics of the oxidation—reduction reactions of the photosystem II quinone acceptor complex, and the pathway for deactivation. FEBS Lett 153:221–226. https://doi.org/10.1016/0014-5793(83)80152-5

Robinson C, Suggett DJ, Cherukuru N et al (2014) Performance of fast repetition rate fluorometry based estimates of primary productivity in coastal waters. J Mar Syst 139:299–310. https://doi.org/10.1016/j.jmarsys.2014.07.016

Samson G, Bruce D (1996) Origins of the low yield of chlorophyll a fluorescence induced by single turnover flash in spinach thylakoids. Biochim Biophys Acta BBA—Bioenerg 1276:147–153. https://doi.org/10.1016/0005-2728(96)00072-2

Samson G, Prášil O, Yaakoubd B (1999) Photochemical and thermal phases of chlorophyll a fluorescence. Photosynthetica 37:163–182. https://doi.org/10.1023/A:1007095619317

Schansker G, Tóth SZ, Strasser RJ (2005) Methylviologen and dibromothymoquinone treatments of pea leaves reveal the role of photosystem I in the Chl a fluorescence rise OJIP. Biochim Biophys Acta BBA—Bioenerg 1706:250–261. https://doi.org/10.1016/j.bbabio.2004.11.006

Schansker G, Tóth SZ, Kovács L et al (2011) Evidence for a fluorescence yield change driven by a light-induced conformational change within photosystem II during the fast chlorophyll a fluorescence rise. Biochim Biophys Acta BBA—Bioenerg 1807:1032–1043. https://doi.org/10.1016/j.bbabio.2011.05.022

Schansker G, Tóth S, Holzwarth A, Garab G (2014) Chlorophyll a fluorescence: beyond the limits of the QA model. Photosynth Res 120:43–58. https://doi.org/10.1007/s11120-013-9806-5

Schödel R, Irrgang K-D, Voigt J, Renger G (1999) Quenching of chlorophyll fluorescence by triplets in solubilized light-harvesting complex II (LHCII). Biophys J 76:2238–2248. https://doi.org/10.1016/S0006-3495(99)77380-7

Schreiber U (1986a) Detection of rapid induction kinetics with a new type of high-frequency modulated chlorophyll fluorometer. Photosynth Res 9:261–272. https://doi.org/10.1007/BF00029749

Schreiber U (2004) Pulse-amplitude-modulation (pam) fluorometry and saturation pulse method: an overview. In: Papageorgiou GC, Govindjee (eds) Chlorophyll a fluorescence: a signature of photosynthesis. Springer, Dordrecht, pp 279–319

Schreiber U, Schliwa U, Bilger W (1986b) Continuous recording of photochemical and non-photochemical chlorophyll fluorescence quenching with a new type of modulation fluorometer. Photosynth Res 10:51–62. https://doi.org/10.1007/bf00024185

Shinkarev V (2004) Photosystem II: oxygen evolution and chlorophyll a fluorescence induced by multiple flashes. In: Papageorgiou G, Govindjee (eds) Chlorophyll a fluorescence. Springer, Dordrecht, pp 197–229

Steffen R, Christen G, Renger G (2001) Time-resolved monitoring of flash-induced changes of fluorescence quantum yield and decay of delayed light emission in oxygen-evolving photosynthetic organisms. Biochemistry 40:173–180

Strasser BJ (1997) Donor side capacity of Photosystem II probed by chlorophyll a fluorescence transients. Photosynth Res 52:147–155. https://doi.org/10.1023/A:1005896029778

Strasser RJ, Srivastava A, Govindjee (1995) Polyphasic chlorophyll a fluorescence transient in plants and cyanobacteria. Photochem Photobiol 61:32–42. https://doi.org/10.1111/j.1751-1097.1995.tb09240.x

Suggett D, Kraay G, Holligan P et al (2001) Assessment of photosynthesis in a spring cyanobacterial bloom by use of a fast repetition rate fluorometer. Limnol Oceanogr 46:802–810

Taoka S, Crofts AR (1990) Two-electron gate in triazine resistant and susceptible *Amaranthus hybridus*. In: Baltscheffsky M (ed) Current research in photosynthesis: Proceedings of the VIIIth international conference on photosynthesis Stockholm, Sweden, August 6–11, 1989. Springer, Dordrecht, pp 547–550

Tomek P, Lazár D, Ilík P, Naus J (2001) Research note: On the intermediate steps between the O and P steps in chlorophyll a fluorescence rise measured at different intensities of exciting light. Funct Plant Biol 28:1151–1160

Tóth SZ, Schansker G, Strasser RJ (2005) In intact leaves, the maximum fluorescence level (FM) is independent of the redox state of the plastoquinone pool: a DCMU-inhibition study. Biochim Biophys Acta BBA—Bioenerg 1708:275–282. https://doi.org/10.1016/j.bbabio.2005.03.012

Tóth SZ, Schansker G, Garab G, Strasser RJ (2007a) Photosynthetic electron transport activity in heat-treated barley leaves: the role of internal alternative electron donors to photosystem II. Biochim Biophys Acta BBA—Bioenerg 1767:295–305. https://doi.org/10.1016/j.bbabio.2007.02.019

Tóth SZ, Schansker G, Strasser RJ (2007b) A non-invasive assay of the plastoquinone pool redox state based on the OJIP-transient. Photosynth Res 93:193. https://doi.org/10.1007/s11120-007-9179-8

Trtilek M, Kramer DM, Koblizek M, Nedbal L (1997) Dual-modulation LED kinetic fluorometer. J Lumin 72–4:597–599. https://doi.org/10.1016/s0022-2313(97)00066-5

Vass I, Kirilovsky D, Etienne AL (1999) UV-B radiation-induced donor- and acceptor-side modifications of photosystem II in the cyanobacterium *Synechocystis* sp. PCC 6803. Biochemistry 38:12786–12794. https://doi.org/10.1021/bi991094w

Vernotte C, Etienne AL, Briantais JM (1979) Quenching of the system II chlorophyll fluorescence by the plastoquinone pool. Biochim Biophys Acta—Bioenerg 545:519–527. https://doi.org/10.1016/0005-2728(79)90160-9